

11, 12

Sensor and Simulation Note

Note 343

1 July 1992

Hyperboloidal Scatterer for Spherical TEM Waves

Carl E. Baum
Phillips Laboratory

Everett G. Farr
Farr Research

Abstract

This paper describes a special hyperboloidal scatterer which can be used as a canonical scatterer in a transient scattering range. It has the property of transforming one spherical TEM wave (from a conical wave launcher) into a second spherical TEM wave with no change in temporal waveform. The amplitude and polarization of the second wave are known analytically in terms of the first. This new solution to Maxwell's equation is useful in the calibration of transient scattering ranges.

CLEARED FOR PUBLIC RELEASE

PL/PA 16 Jul 92

PL 92 -0505

I. Introduction

In [2] it was shown that an inhomogeneous TEM plane wave, axially incident on a perfectly conducting paraboloid (of revolution) scatters as an outgoing spherical TEM wave centered on the paraboloidal focus. In this case the paraboloid is curved away from the incident wave. It is to be noted that the solution of the Maxwell equations and boundary conditions is exact, not just an approximation (e.g. for high frequency). This solution applies directly in time domain up to some "clear time" when the waves encounter some scatterer (e.g. truncation of the paraboloid, or the spherical TEM wave encountering the guiding conductors of the plane TEM wave) and reach the observer at a time subject to the speed-of-light limitation (causality). Reversing the propagation (time-reversal symmetry if you like) of course makes this solution apply for an incoming inhomogeneous TEM wave scattering into a plane wave propagating away from the paraboloid.

This solution is closely related to the case in [1] where an outgoing spherical TEM wave (from a paraboloidal focus) scatters from the paraboloidal reflector (concave to the source), giving a plane TEM wave (inhomogeneous). This is also an exact solution of the Maxwell equations, applying up to times when other scattering enters into the fields at positions of interest. This case applies to part of the design of the reflector type of IRA (impulse radiating antenna).

This paper extends the exact scattering results to the case when both incident and scattered fields are inhomogeneous spherical TEM waves. An outgoing spherical wave scattering into an outgoing spherical wave (or incoming to incoming by reciprocity) gives the case of one sheet of a hyperboloid of revolution as the scatterer. Both spherical waves are centered on the axis of revolution.

Although this new solution to Maxwell's equations is interesting in its own right, it is of particular interest to the problem of scattering range calibration. In [2] it was shown that a paraboloid made an excellent scatterer for calibration purposes, however, it was necessary to have a transmitter a long distance away in order for the phase front to be planar at the scatterer. With this new solution, we can now identify a hyperboloid as the correct canonical scatterer which does take into account the spherical shape of the incident phase front. Furthermore, one now has the capability to calibrate accurately a geometry where the transmitter must be close to the scatterer.

II. Double Stereographic Transformation

As is well known [4] there exist solutions of the Maxwell equations in the form of spherical TEM waves. Referring to fig. 1 we have such a wave (wave 1) propagating away from $(x, y, z) = (0, 0, z_{10})$. In spherical coordinates (r_1, θ_1, ϕ_1) centered on this point (with $\theta_1 = 0$ pointing along the negative z axis) we have the electric field in the form

$$\vec{E}_1 = \frac{-1}{r_1} \nabla_{\theta_1, \phi_1} V_1(\theta_1, \phi_1) f\left(t - \frac{r_1 - \ell_1}{c}\right) \quad (2.1)$$

where zero time has been set by first wave arrival at the reflector (on the z axis). Here the transverse gradient is on the unit sphere as

$$\nabla_{\theta_1, \phi_1} = \bar{1}_{\theta_1} \frac{\partial}{\partial \theta_1} + \bar{1}_{\phi_1} \frac{1}{\sin(\theta_1)} \frac{\partial}{\partial \phi_1} \quad (2.2)$$

Such a wave is launched by a small source (at the origin of the \bar{r}_1 coordinates) connected to two or more (perfectly) conducting cones (of arbitrary cross section) described in terms of θ_1, ϕ_1 coordinates. In practice such cones have finite length but it takes some time after wave arrival at a particular position for the truncation to be noticed.

The potential satisfies the Laplace equation on the unit sphere

$$\begin{aligned} \nabla_{\theta_1, \phi_1}^2 V_1(\theta_1, \phi_1) &= 0 \\ \nabla_{\theta_1, \phi_1}^2 &= \frac{1}{\sin(\theta_1)} \frac{\partial}{\partial \theta_1} \sin(\theta_1) \frac{\partial}{\partial \theta_1} + \frac{1}{\sin^2(\theta_1)} \frac{\partial^2}{\partial \phi_1^2} \end{aligned} \quad (2.3)$$

with constant potentials on each of the conducting cones. Using cylindrical coordinates (Ψ, ϕ, z) with

$$x = \Psi \cos(\phi) \quad , \quad y = \Psi \sin(\phi) \quad (2.4)$$

the stereographic transformation takes the form

$$\begin{aligned} \Psi_o &= 2\ell_1 \tan\left(\frac{\theta_1}{2}\right) \\ \phi_o &= -\phi_1 \end{aligned} \quad (2.5)$$

where Ψ_o and ϕ_o are now polar coordinates on a plane perpendicular to the z axis at $-L$. Points on sphere 1 of radius ℓ_1 are mapped by projection from a point on the z axis at $z_{10} + \ell_1$ onto this stereographic projection plane (which is also tangent to the sphere). Near the z axis the

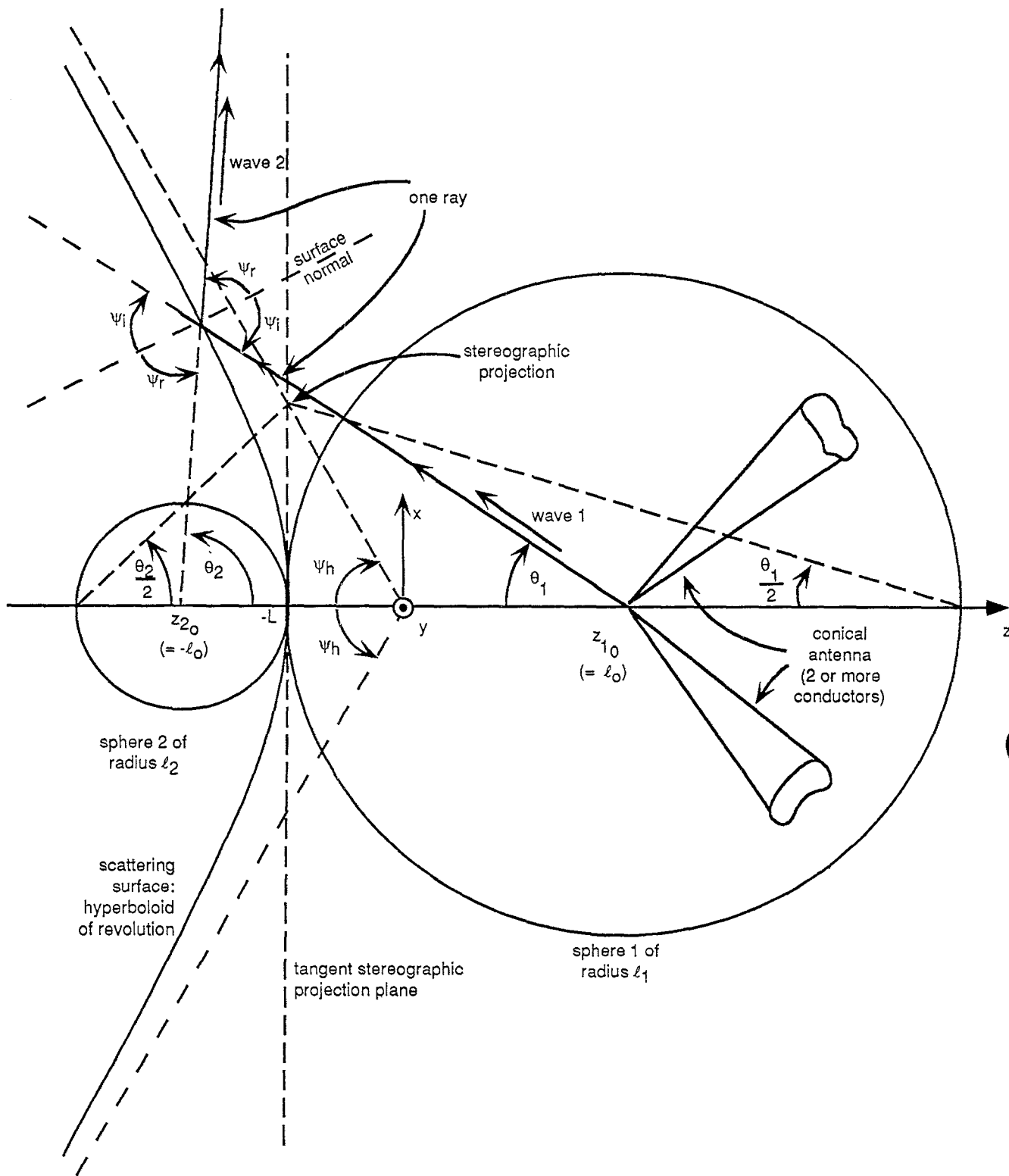


Fig. 1. Reflector with Two Outward-Propagating Spherical TEM Waves

coordinates on the projection plane closely match those on the sphere, but this is distorted as θ_1 increases from zero. In terms of these new equivalent cylindrical coordinates the potential also satisfies the Laplace equation (on the projection plane) as

$$\begin{aligned} \nabla_{\Psi_o, \phi_o}^2 V_1(\theta_1, \phi_1) &= 0 \\ \nabla_{\Psi_o, \phi_o} &= \bar{1}_{\Psi_o} \frac{\partial}{\partial \Psi_o} + \bar{1}_{\phi_o} \frac{\partial}{\partial \phi_o} \\ \nabla_{\Psi_o, \phi_o}^2 &= -\frac{1}{\Psi_o} \frac{\partial}{\partial \Psi_o} \Psi_o \frac{\partial}{\partial \Psi_o} + \frac{1}{\Psi_o^2} \frac{\partial^2}{\partial \phi^2} \end{aligned} \quad (2.6)$$

Mapping the conical boundaries onto the projection plane (via their intersection with sphere 1) gives an equivalent two-dimensional problem which can be solved by various techniques, including conformal transformation. As many such geometries have known solutions, the stereographic transformation allows one to apply these to systems of conical conductors related by (2.5). The solution here then applies to any spherical TEM wave with an analytic representation, potentially a large list.

Consider now a second spherical TEM wave (outgoing) centered on $(x, y, z) = (0, 0, z_{2o})$ as

$$\bar{E}_2 = \frac{-1}{r_2} \nabla_{\theta_2, \phi_2} V_2(\theta_2, \phi_2) f\left(t - \frac{r_2 - \ell_2}{c}\right) \quad (2.6)$$

which has the same waveform f , and same arrival time (zero) at the reflector on the z axis. Both waves are considered to the right of the reflector for present purposes. However, there is a similar solution for both waves to the left.

In terms of the second spherical coordinate system (r_2, θ_2, ϕ_2) all the previous results can be applied to this wave as well. Now the stereographic transformation reads

$$\begin{aligned} \Psi_o &= 2\ell_2 \tan\left(\frac{\theta_2}{2}\right) \\ \phi_o &= \phi_2 \end{aligned} \quad (2.7)$$

where now sphere 2 of radius ℓ_2 is used for the projection from a point on the z axis at $z_{2o} - \ell_o$. Note that both spheres are tangent to the same projection plane at $z = -L$.

As Interpreted geometrically in fig. 1, both spherical waves are mapped onto the same plane. This allows one to map from one set of spherical coordinates to the second via

$$2\ell_2 \tan\left(\frac{\theta_2}{2}\right) = \Psi_o = 2\ell_1 \tan\left(\frac{\theta_1}{2}\right) \quad (2.8)$$

$$\phi_2 = \phi_o = -\phi_1$$

which one can call a double stereographic transformation. Potentials V_1 appropriate to spherical TEM wave 1 satisfy the Laplace equation (transverse) in \bar{r}_1 coordinates. Via (2.8) such potentials satisfy the Laplace equation on the projection plane, and then on a sphere (transverse) in the \bar{r}_2 system. So for any acceptable V_1 there is an acceptable V_2 as a constant times V_1 . In

particular let us choose

$$V_2(\theta_2, \phi_2) = -V_1(\theta_1, \phi_1) \quad (2.9)$$

Together with (2.8) this can be referred to as a hyperboloidal reflector transform as we shall later see.

III. Hyperboloid from Matching Time on Surface

In fig. 1 consider a ray corresponding initially to wave 1 with angle θ_1 . Due to the rotational symmetry this can be taken for illustration with $\theta_1 = 0$, but the results apply for all ϕ_1 . This ray passes through sphere 1 (at a point which is stereographically projected to the $z = -L$ plane) and continues on until it meets the reflector where it meets (and is reflected into) a ray corresponding to wave 2 at angle θ_2 . There are various things to be considered to show how the boundary condition (zero tangential electric field) is satisfied on the scatterer. In this section let us first establish the reflector shape as (one of two sheets of) a hyperboloid of revolution.

Matching the time portion of the two waves on the surface we set

$$f\left(t - \frac{r_{1h} - \ell_1}{c}\right) = f\left(t - \frac{r_{2h} - \ell_2}{c}\right) \quad (3.1)$$

from (2.1) and (2.6). Here a subscript "h" is used to denote coordinates on the scattering surface. For arbitrary waveforms we then have

$$r_{1h} - \ell_1 = r_{2h} - \ell_2 \quad (3.2)$$

with the relations

$$\ell_1 + \ell_2 \equiv 2\ell_o, \quad \ell_1 - \ell_2 \equiv 2L \quad (3.3)$$

we have

$$r_{1h} - r_{2h} = 2L \quad (3.4)$$

which is one way to describe the hyperboloid, the points $\pm\ell_o$ on the z axis being the two foci.

Points on this hyperboloid have a constant difference ($2L$) in the distance from the two foci.

Now derive an equation in cylindrical coordinates (ϕ independent) appropriate to this body of revolution. From (3.4) we have

$$\left[\Psi_h^2 + (\ell_o - z_h)^2\right]^{\frac{1}{2}} = \left[\Psi_h^2 + (\ell_o + z_h)^2\right]^{\frac{1}{2}} + 2L \quad (3.5)$$

which when squared and terms canceled gives

$$\left[\Psi_h^2 + (\ell_o + z_h)^2\right]^{\frac{1}{2}} = \frac{-\ell_o}{L} z_h - L \quad (3.6)$$

which can be squared again and terms canceled to give

$$\left[\left(\frac{\ell_o}{L} \right)^2 - 1 \right] z_h^2 - \Psi_h^2 = \ell_o^2 - L^2 \quad (3.7)$$

Normalizing the coordinates gives the canonical form

$$\left(\frac{z_h}{L} \right)^2 - \frac{\Psi_h^2}{\ell_o^2 - L^2} = 1 \quad (3.8)$$

As indicated in fig. 1 there is a cone of half-angle ψ_h which is asymptotic to the hyperboloid as

$$\psi_h = \lim_{\Psi_h \rightarrow \infty} \arctan \left(-\frac{\Psi_h}{z_h} \right) = \arctan \left(\left[\left(\frac{\ell_o}{L} \right)^2 - 1 \right]^{\frac{1}{2}} \right) \quad (3.9)$$

Here we take the solution for negative z since we have assumed L negative. If L is positive the solution for positive z is appropriate.

At this point one can note that the equal-time constraint automatically makes the ray scatter from the surface (in a high-frequency sense) with

$$\begin{aligned} \psi_r &= \psi_i \\ \psi_i &\equiv \text{incidence angle} \\ \psi_r &\equiv \text{reflection angle} \end{aligned} \quad (3.10)$$

These angles are taken with respect to the local surface normal in fig. 1.

IV. Equivalence of Double Transform and Angle Matching on Hyperboloid

The transform (double stereographic) in (2.8) relates θ_1 and θ_2 . Fig. 1 shows the usual geometric interpretation of the two stereographic transforms on the $z = -L$ plane. However, one would like to relate this to the idea of the rays at angles θ_1 and θ_2 meeting on the hyperboloid.

So let us consider this geometric problem.

Assuming the two rays meet on the hyperboloid we have

$$\begin{aligned} r_{1h} \cos(\theta_{1h}) + r_{2h} \cos(\theta_{2h}) &= 2\ell_o \\ \frac{\sin(\theta_{1h})}{r_{2h}} &= \frac{\sin(\theta_{2h})}{r_{1h}} = \frac{\sin(\theta_{1h} + \theta_{2h})}{2\ell_o} \quad (\text{law of sines}) \\ r_{1h} - r_{2h} &= 2L \end{aligned} \quad (4.1)$$

Substituting from the second of these into the third gives

$$\begin{aligned} r_{1h} &= 2L \left[1 - \frac{\sin(\theta_{1h})}{\sin(\theta_{2h})} \right]^{-1} \\ r_{2h} &= -2L \left[1 - \frac{\sin(\theta_{2h})}{\sin(\theta_{1h})} \right]^{-1} \end{aligned} \quad (4.2)$$

with the two radii now expressed in terms of the two angles. Substituting these results into the first of (4.1) gives

$$2L \frac{\sin(\theta_{2h}) \cos(\theta_{1h})}{\sin(\theta_{1h}) - \sin(\theta_{2h})} - 2L \frac{\cos(\theta_{2h}) \sin(\theta_{1h})}{\sin(\theta_{1h}) - \sin(\theta_{2h})} = 2\ell_o \quad (4.3)$$

which can be manipulated into the form

$$\frac{1 - \frac{L}{\ell_o} \cos(\theta_{1h})}{\sin(\theta_{1h})} = \frac{1 + \frac{L}{\ell_o} \cos(\theta_{2h})}{\sin(\theta_{2h})} \quad (4.4)$$

This is a relation between θ_{1h} and θ_{2h} coordinates only.

To compare (4.4) with the double stereographic transform first use [3]

$$\begin{aligned}\sin(\theta) &= \frac{2 \tan\left(\frac{\theta}{2}\right)}{1 + \tan^2\left(\frac{\theta}{2}\right)} \\ \cos(\theta) &= \frac{1 - \tan^2\left(\frac{\theta}{2}\right)}{1 + \tan^2\left(\frac{\theta}{2}\right)}\end{aligned}\tag{4.5}$$

Substituting for both θ_{1h} and θ_{2h} in (4.4) we find

$$\begin{aligned}& \frac{1 - \frac{L}{\ell_o}}{2 \tan\left(\frac{\theta_{1h}}{2}\right)} + \frac{1 + \frac{L}{\ell_o}}{2} \tan\left(\frac{\theta_{1h}}{2}\right) \\ &= \frac{1 + \frac{L}{\ell_o}}{2 \tan\left(\frac{\theta_{2h}}{2}\right)} + \frac{1 - \frac{L}{\ell_o}}{2} \tan\left(\frac{\theta_{2h}}{2}\right)\end{aligned}\tag{4.6}$$

Now the double stereographic transform from (2.8) is

$$2[\ell_o + L] \tan\left(\frac{\theta_1}{2}\right) = 2[\ell_o - L] \tan\left(\frac{\theta_2}{2}\right)\tag{4.7}$$

This is equivalent to

$$\frac{1 + \frac{L}{\ell_o}}{2} \tan\left(\frac{\theta_1}{2}\right) = \frac{1 - \frac{L}{\ell_o}}{2} \tan\left(\frac{\theta_2}{2}\right)\tag{4.8}$$

and to

$$\frac{1 - \frac{L}{\ell_o}}{2 \tan\left(\frac{\theta_1}{2}\right)} = \frac{1 + \frac{L}{\ell_o}}{2 \tan\left(\frac{\theta_2}{2}\right)}\tag{4.9}$$

Adding (4.8) and (4.9) and identifying

$$\theta_1 \equiv \theta_{1h} \quad , \quad \theta_2 \equiv \theta_{2h}\tag{4.10}$$

gives (4.6). Therefore the double stereographic transform (4.7) implies that θ_1 and θ_2 match on the hyperboloidal boundary.

V. Matching Potentials and Fields on Hyperboloid

Now that the waveforms match on the hyperboloid in (3.1), and the double stereographic transform has θ_1 and θ_2 (and $\phi_1 = -\phi_2$) matching on the boundary, look at (2.9) where the potentials are chosen to match as

$$V_2(\theta_{2h}, \phi_{2h}) = -V_1(\theta_{1h}, \phi_{1h}) \quad (5.1)$$

Viewed another way the potentials sum to zero at each point on the boundary. However, these are potentials corresponding to the transverse fields in two different spherical coordinate systems.

Consider the resulting tangential electric field on the boundary as specified from the sum of (2.1) and (2.6). There are two tangential components to be considered as in [2]. Here we have for the ϕ component (or the \bar{I}_{h1} direction)

$$\begin{aligned} E_{1\phi_h} &= -E_{1\phi_{1h}} = \frac{1}{r_{1h} \sin(\theta_{1h})} \frac{\partial}{\partial \phi_{1h}} V_1(\theta_{1h}, \phi_{1h}) f\left(t - \frac{r_{1h} - \ell_1}{c}\right) \\ &= -\frac{1}{\Psi_h} \frac{\partial}{\partial \phi} V_1(\theta_{1h}, \phi_{1h}) f\left(t - \frac{r_{1h} - \ell_1}{c}\right) \\ E_{2\phi_h} &= -\frac{1}{r_{2h} \sin(\theta_{2h})} \frac{\partial}{\partial \phi_{2h}} V_2(\theta_{2h}, \phi_{2h}) f\left(t - \frac{r_{2h} - \ell_1}{c}\right) \\ &= -\frac{1}{\Psi_h} \frac{\partial}{\partial \phi} V_2(\theta_{2h}, \phi_{2h}) f\left(t - \frac{r_{2h} - \ell_1}{c}\right) \end{aligned} \quad (5.2)$$

From (3.1) and (5.1) we directly have

$$E_{1\phi_h} + E_{2\phi_h} = 0 \quad (5.3)$$

The second tangential component is taken in the \bar{I}_{h2} direction. This is normal to $\bar{I}_{h1} = \bar{I}_\phi$ and is in the x,z plane for the case of $\phi = 0$ illustrated in fig.1. For wave 1 there is no component in the r_1 direction and similarly for wave 2. Projecting the θ_1 and θ_2 components gives

$$\begin{aligned} \bar{I}_{h2} \cdot \bar{E}_{1h} &= -\frac{\cos(\psi_i)}{r_{1h}} \frac{\partial}{\partial \theta_{2h}} V_1(\theta_{1h}, \phi_{1h}) f\left(t - \frac{r_{1h} - \ell_1}{c}\right) \\ \bar{I}_{h2} \cdot \bar{E}_{2h} &= -\frac{\cos(\psi_r)}{r_{2h}} \frac{\partial}{\partial \theta_{2h}} V_2(\theta_{2h}, \phi_{1h}) f\left(t - \frac{r_{2h} - \ell_2}{c}\right) \end{aligned} \quad (5.4)$$

Now along the hyperboloid in the \bar{I}_{h2} direction we have a differential length

$$d\ell = \frac{r_{1h} d\theta_{1h}}{\cos(\psi_i)} = \frac{r_{2h} d\theta_{2h}}{\cos(\psi_r)} \quad (5.5)$$

Together with (3.1) and (5.1) this gives

$$\bar{1}_{h2} \cdot [\bar{E}_{1h} + \bar{E}_{2h}] = 0 \quad (5.6)$$

The net-zero tangential electric field on the hyperboloid can be simply viewed from another perspective. Since (5.1) shows that the sum of the two transverse potentials is zero everywhere on the surface, and since the tangential electric field is given by the derivatives of these potentials along the surface, then the net tangential electric field is directly zero. Since the waves satisfy not only the Maxwell equations but also the boundary conditions, we have found the unique solution.

In calculating the waves, the second can be readily related to the first through the values on the hyperboloid. The first wave being given as in (2.1), this takes the given incident field which we write as

$$\begin{aligned} \bar{E}_1 &= \bar{E}_{1o}(\theta_{1h}, \phi_{1h}) f\left(t - \frac{r_{1h} - \ell_1}{c}\right) \\ \bar{E}_{1o}(\theta_{1h}, \phi_{1h}) &= -\frac{1}{r_{1h}} \left[\nabla_{\theta_1, \phi_1} V_1(\theta_1, \phi_1) \right] \Bigg|_{\substack{\theta_1 = \theta_{1h} \\ \phi_1 = \phi_{1h}}} \\ &= E_{1\theta_{1h}} \bar{1}_{\theta_{1h}} + E_{1\phi_{1h}} \bar{1}_{\phi_{1h}} \end{aligned} \quad (5.7)$$

The second wave has the general form in the second spherical coordinate system

$$\begin{aligned} \bar{E}_2 &= \frac{r_{2h}}{r_2} \bar{E}_{2o}(\theta_{2h}, \phi_{2h}) f\left(t - \frac{r_2 - \ell_2}{c}\right) \\ \bar{E}_{2o}(\theta_{2h}, \phi_{2h}) &= -\frac{1}{r_{2h}} \left[\nabla_{\theta_2, \phi_2} V_2(\theta_2, \phi_2) \right] \Bigg|_{\substack{\theta_2 = \theta_{2h} \\ \phi_2 = \phi_{2h}}} \\ &= E_{2\theta_{2h}} \bar{1}_{\theta_{2h}} + E_{2\phi_{2h}} \bar{1}_{\phi_{2h}} \end{aligned} \quad (5.8)$$

Matching the tangential fields of the boundary gives

$$\begin{aligned} E_{2\theta_{2h}} &= -E_{1\theta_{1h}} \\ E_{2\phi_{2h}} &= E_{1\phi_{1h}} \end{aligned} \quad (5.9)$$

noting the opposite senses of ϕ_1 and ϕ_2 . Thus the second wave has field component which are extrapolated by r_{2h}/r_2 (as one moves away from the hyperboloid) in terms of the field components of the first wave at the hyperboloid.

VI. Concluding Remarks

The solution here is quite general. There are many forms the first spherical TEM wave can take, depending on the conical antenna used to launch it. For all such waves the second spherical TEM wave can be directly constructed via the double stereographic transform. Since the requisite shape of the scatterer is one sheet of a hyperboloid of revolution, one can think of this transform as the hyperboloidal transform.

The solution, while exact, only applies for limited time. A practical scatterer is truncated, the truncation serving as a scatterer which sends fields to an observer, cutting off the time for which the solution can be used. (See fig. 3 of [2] for this geometry in the similar case of a paraboloid.) As in fig. 1 the presence of the conical antenna also serves as a scatterer of wave 2, sending a signal which is eventually received by the observer. Furthermore the finite length of the conical antenna means that wave 1 scatters from the truncation of the cones, also propagating to the observer. All of these additional scattered waves need to be considered when computing the time window of solution applicability. Turning this around one can design the conical antenna and hyperboloid to give a desired time window.

References

1. E.G. Farr and C.E. Baum, Prepulse Associated with the TEM Feed of an Impulse Radiating Antenna, Sensor and Simulation Note 337, March 1992.
2. E.G. Farr and C.E. Baum, A Canonical Scatterer for Transient Scattering Range Calibration, Sensor and Simulation Note 342, June 1992.
3. M. Abramowitz and I.A. Stegun, Handbook of Mathematical Functions, AMS-55, U.S. Gov't Printing Office, 1964.
4. W.R. Smythe, Static and Dynamic Electricity, Hemisphere Publishing Corp., 1989.